J Mater Sci (2013) 48:1524–1532
DOI 10.1007/s10853-012-6907-z

Glycolic acid-functionalized chitosan–Co_3O_4–Fe_3O_4 hybrid magnetic nanoparticles-based nanohybrid scaffolds for drug-delivery and tissue engineering

Sangeeta Kumari · Raj Pal Singh

Received: 11 April 2012 / Accepted: 18 September 2012 / Published online: 4 October 2012

Abstract In the present work, Co_3O_4 was prepared by hydrothermal process, which is further used for the synthesis of Co_3O_4–Fe_3O_4 hybrid nanoparticles. The formation of Co_3O_4–Fe_3O_4 nanoparticles was investigated by transmission electron microscopy and physical property measurement system. In the next step, the drug-loaded novel nanohybrid porous scaffold based on chitosan-g-glycolic acid and Co_3O_4–Fe_3O_4 nanoparticle was prepared by freeze drying technique. The grafting of glycolic acid on chitosan drug loading in porous scaffold was characterized by Fourier transform infrared spectroscopy. The nanohybrid scaffolds were found to be stable regardless of the pH of the medium and play an important role in cell adhesion, proliferation, and migration. Co_3O_4–Fe_3O_4 hybrid nanoparticles' reinforcement was found to control the drug (cyclophosphamide) release rate in phosphate buffer saline solution (pH 7.4). Therefore, Co_3O_4–Fe_3O_4 hybrid nanoparticles are viable additives for formulating sustained drug delivery systems and could be applied in the field of biomaterials.

Electronic supplementary material The online version of this article (doi:10.1007/s10853-012-6907-z) contains supplementary material, which is available to authorized users.

S. Kumari
Division of Polymer Science and Engineering, National Chemical Laboratory, Dr. Homi Bhabha Road, Pune 411 008, Maharashtra, India

R. P. Singh (✉)
Advanced Research Centre in Pharmaceutical Sciences & Applied Chemistry, Bharati Vidyapeeth University, Erandawane, Pune 411 038, Maharashtra, India
e-mail: rp.singh.ncl@gmail.com

Introduction

In the field of nanotechnology, polymer matrix-based nanocomposites have become a prominent area of current research and development. These materials exhibit unique optical [1], thermal, electrical, and mechanical properties due to the interaction of the polymer with the particle and state of dispersion [2–4]. Transition metal nanoparticles are one of the most studied systems due to their quantum size effects [5–7], novel electronic [8], optical [9], magnetic [10], and chemical properties. These metal nanoparticles play an important role in many different fields of science such as nanoelectronics, catalysis [11–13], and, recently, in biomedical application [14–16]. Cobalt oxide and Fe_3O_4 nanoparticles are currently attracting enormous interest owing to their unique size- and shape-dependent properties and potential applications in the field of catalysis, sensors, electrochemistry, magnetism, energy storage, etc. [17]. Here, we have demonstrated that Co_3O_4–Fe_3O_4 composite magnetic nanoparticle-based materials can be use in the field of controlled drug release and cell proliferation systems which are having major scientific applications in the field of biomaterials [18].

A wide range of materials have been employed as drug carriers such as lipids, surfactant, dendrimers, and natural or synthetic polymers [19–22]. Chitosan has prompted the continuous movement for the development of safe and effective drug delivery systems because of its unique physicochemical and biologic characteristics. Chitosan, *a* (1–4) 2-amino-2-deoxy-b-D glucan, has structural characteristics similar to glycosaminoglycans. This polycationic biopolymer is generally obtained by alkaline deacetylation of chitin, which is the main component of the exoskeleton of crustaceans [23] Chitosan is hydrophilic and compatible with nanoparticle and has better processability

due to the presence of amino group (pKa value is 6.2) in the chain. Chemical modification of chitosan is useful for the association of bioactive molecules to polymer and controlling the drug release profile. The grafting of side glycolic acid leads to marked changes in the chitosan structure [24, 25]. Chitosan has amino and hydroxyl functional group which act as potential site for altering the polymers functionality [26–28].

In this paper, we have synthesised Co_3O_4–Fe_3O_4 composite magnetic nanoparticles. These Co_3O_4–Fe_3O_4 composite nanoparticles were dispersed into the matrix of glycolic acid-grafted chitosan scaffolds, which are prepared using lyophilizer by freeze drying. This novel nanohybrid scaffold of chitosan-g-glycolic acid embedded with Co_3O_4–Fe_3O_4 composite magnetic nanoparticles can be used in the field of controlled drug delivery and tissue engineering applications.

Experimental

Materials

Chitosan of low molecular weight (Mw = 1.5×10^5, degree of deacetylation was 85 %), glycolic acid (99 % pure), iron (0) pentacarbonyl ($Fe(CO)_5$), oleic acid (OA), oleylamine (OAM), cobalt acetate ($Co(OAc)_2$), and citric acid ($C_6H_8O_7$) were obtained from Sigma-Aldrich. Lithium chloride (LiCl), tri phenyl phosphate (TPP), pyridine (Py), sodium hydroxide (NaOH), and phenyl ether were obtained from M/s Sisco Research Laboratories, Mumbai. Deionised water was used throughout the work, which is prepared by Milli-Q-system.

Synthesis of cobalt oxide (Co_3O_4) nanoparticles (CoNP)

CoNP were prepared by hydrothermal method. In which, cobalt acetate, citric acid, and NaOH (1:1:2) ratio was put into hydrothermal bomb containing 110 mL of water. The hydrothermal bomb was screw tight and heated at 120 °C for 40 h. The formed precipitate was centrifuged and separated. Further, the precipitate was calcinated at 350 °C for 24 h. After calcination, the precipitate was cooled at room temperature.

Synthesis of Co_3O_4–Fe_3O_4 hybrid nanoparticles (CFNP)

CoNP, 1-octadecene, OAM, and OA were heated to 120 °C under argon atmosphere. At the temperature of 120 °C, $Fe(CO)_5$ was injected to the reaction mixture. The reaction mixture was slowly heated to reflux (1 °C min^{-1}) for 4.5 h. After the completion of the reaction, it is cooled to room temperature and stirred for 1 h, followed by precipitation with acetone. The precipitate was then dried in air.

Grafting of chitosan with glycolic acid

Grafting of glycolic acid on chitosan was achieved by click reaction. Chitosan (1 g) and glycolic acid (1 g) were taken in a round bottom flask. TPP, LiCl, and Py in 1:1:1 ratio was added to the round bottom flask. To the reaction mixture, 12 mL of *N*-methyl pyrilidone (NMP) was added. The reaction mixture was stirred and refluxed for 8 h at 120 °C. After 8 h, the viscous reaction mixture was cooled to room temperature and precipitated with methanol. The precipitate was dried at 70 °C for 10 h under reduced pressure.

Preparation of nanohybrid scaffolds and drug loading

Glycolic acid-grafted chitosan (1 g) was dispersed in deionised water (50 mL) and stirred for 1 h at room temperature. After 1 h, Co_3O_4–Fe_3O_4 composite magnetic nanoparticles (50 mg) were added to the solution and stirred overnight at room temperature. The resulting solution was heated up to 80 °C with continuous degassing for 30 min. The resulting solution was cooled to room temperature after degassing. The drug (CPA) (10 mg) was added to the resulting solution and stirred for 5 h so that the drug completely mixes with the solution. The drug-loaded solution was poured in tissue culture plates (20 × 20 mm diameter) and quenched in liquid nitrogen. The quenched sample was freeze dried by lyophilization under −100 °C temperature for 6 h. In lyophilization, the water molecules were removed by freezing and sublimation of ice crystals, which lead to the formation of pores. The formulation is shown in the Table 1.

Characterizations

High resolution transmission electron microscopy (HR-TEM model Technai TF30, 300 kV FEG) was used to analyze the particle size, morphology, and Selected Area Diffraction pattern (SAED) of Co_3O_4–Fe_3O_4 hybrid magnetic nanoparticles. The formation of Co_3O_4–Fe_3O_4 hybrid nanoparticle was confirmed by measuring hysteresis loops of the synthesised nanoparticles using a physical property measuring system (PPMS) (quantum design Inc. San Diego, USA) equipped with 7T superconducting magnet and a vibrating sample magnetometer [29]. Attenuated total reflectance Fourier transform infrared (ATR-FTIR) Nicolet Nexus 870 FTIR spectrometer equipped with a smart Endurance diamond accessory (64 scans, 4 cm^{-1} resolution, wave number range 4000–550 cm^{-1}) was used

Table 1 Formulation of cyclophosphamide (CPA)-loaded nanohybrid of chitosan-g-glycolic acid and Co_3O_4–Fe_3O_4 hybrid magnetic nanoparticles

S. no.	Grafted chitosan (g)	Co_3O_4–Fe_3O_4 (mg)	CPA (%)	Drying process	Sample code
1	1	–	–	Vacuum	CGCF-1
2	1	50	–	Vacuum	CGCF-2
3	1	50	–	Freeze	CGCF (S)
4	1	50	10	Freeze	CGCF (D)

to analyze fourier transform infrared spectra of neat chitosan (CTS), chitosan grafted glycolic acid (CGCF-1), nanohybrid scaffold (CGCF-(D)), and cyclophosphamide (CPA) drug. XRD patterns of the samples were recorded on X-ray Diffractometer (WAXRD—Rigaku (Japan)) with Cu-kα radiation at a voltage of 50 kV. The scanning rate was 4° min^{-1} and the scanning scope of 2θ was from 2 to 80° at room temperature. Scanning electron microscopy (SEM) (Model, JOEL Stereoscan 440, Cambridge) was used to investigate the surface morphology of the porous scaffolds. Before the observation, specimens were fixed on the copper grid. The swelling behavior of porous scaffold was determined by exposing them to media of different pH—1 N HCl, 1 N NaOH, and simulated body fluid (SBF) (pH 7.4) solutions. The shape retention of porous scaffold was determined by measuring the change in its diameter of scaffold as a function of time in the media. The drug-loaded nanohybrid scaffold (CGCF-(D)) was immersed in aliquots of 0.1 M sodium phosphate buffer (pH 7.4) and incubated at 37 °C. An aliquot of 3 mL from the specimen was withdrawn after specific time interval and immediately fresh medium is added to it. The "CPA" content in the aliquot was investigated using UV–vis spectrophotometer (UV-NIR- PL Lamda 950) at 180 nm. In vitro cell culture was carried out using L929 cell. These cells are derived from mouse fibroblast cell line and are internationally recognized cells which are routinely used in in vitro cytotoxicity assessments. The scaffold was sterilised by putting it in 6-well tissue culture plate containing isopropanol (5 mL) and exposed to UV radiation for 4 h. L929 cells were further seeded on nanohybrid scaffold placed in 6-well plate at a density of 5×10^3 cells/well and incubated at 37 °C, 5 % CO_2, and 95 % humidity incubation conditions. The tissue culture plate containing only cells were used as control. To study the cell proliferation on different substrates, cell proliferation was determined by the colorimetric MTT assay. MTT assay is based on the reduction of yellow 3-(4,5 dimethylthiazol-2-yl)-2, 5-diphenyltetrazolium bromide (MTT) salt in MTT to form purple formazan by dehydrogenase enzymes secreted from the mitochondria of metabolically active cells. The amount of formazan formed is directly proportional to the number of viable cells. After 2, 4, 6, 24, 48, and 72 h, the cell solution (100 µL) was transferred to an ELISA microplate and optical density (OD) was measured at 540 nm by the spectroscopic method [30]. The relative cell growth was compared to the control cells, which exhibit cell culture medium without chitosan. It was calculated by the given Eq. (1)

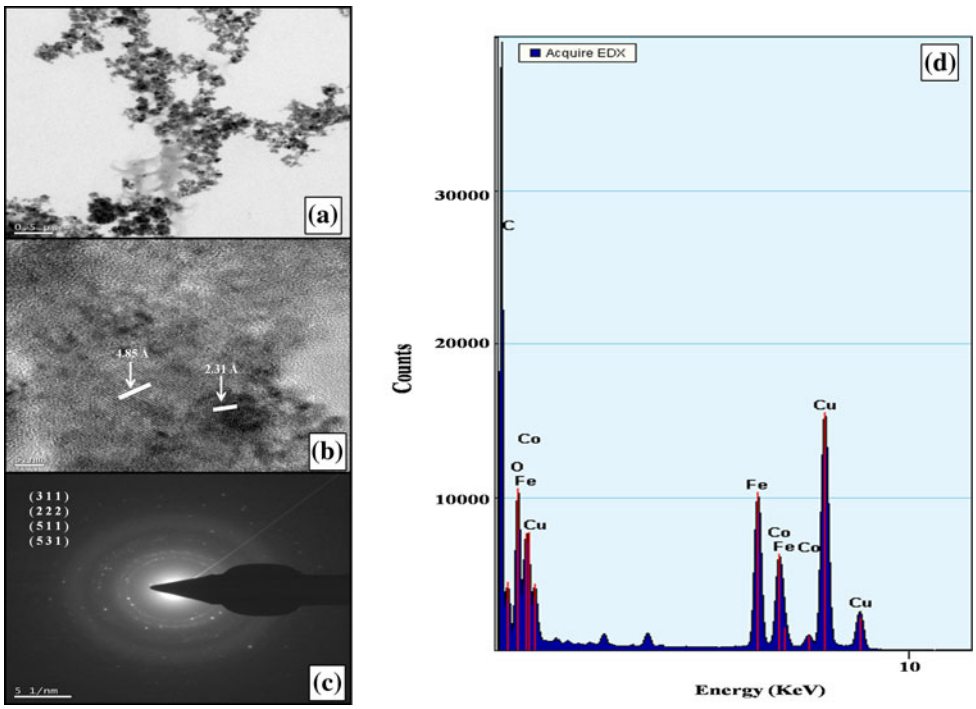

Fig. 1 **a** TEM image Co_3O_4–Fe_3O_4 hybrid nanoparticles; **b** HRTEM image of Co_3O_4–Fe_3O_4 hybrid nanoparticles (*white line* delineate distance between two lattice plane in Co_3O_4 domain and Fe_3O_4 domain); **c** SAED pattern of Co_3O_4–Fe_3O_4 hybrid nanoparticles; **d** TEM-EDAX of Co_3O_4–Fe_3O_4 hybrid nanoparticles

$$\%\,\text{Livecell} = 100 - \left[\frac{(C-T)}{(C-B)} \times 100\right] \quad (1)$$

C = OD of control, T = OD of test sample, B = OD of blank, OD = optical density.

All the in vitro tests were done in triplicate and the results were reported as an average value.

Results and discussion

TEM analysis of Co_3O_4–Fe_3O_4 hybrid nanoparticles

The TEM image of Co_3O_4–Fe_3O_4 composite magnetic nanoparticles (Fig. 1a) exhibits uniformly spherical morphology almost same overall size. Figure 1b shows the high resolution TEM image of these composite magnetic nanoparticles, which are crystalline as shown in the selected area diffraction (SAED) pattern Fig. 1c. The distance between the two adjacent lattice planes in Co_3O_4 domain is 2.31 Å, which is close to the reported value of 2.33 Å for (2 2 2) plane [28], and that in Fe_3O_4 domains 4.85 Å, which is close to the literature value of 4.88 Å for (1 1 1) plane. TEM-EDAX also confirms the formation of Co_3O_4–Fe_3O_4 hybrid nanoparticles (Fig. 1d).

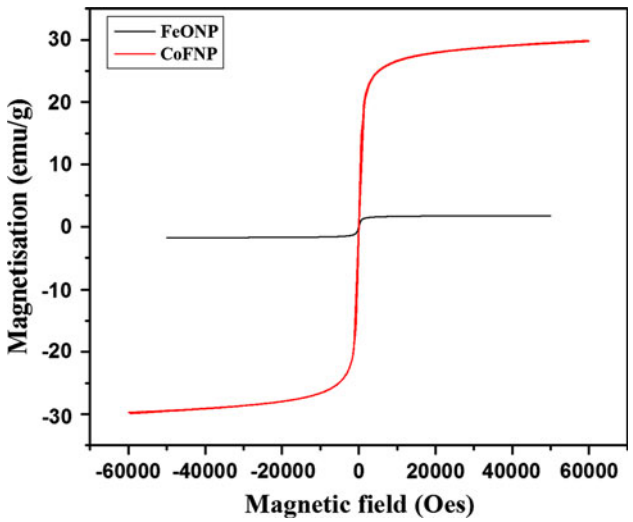

Fig. 2 Magnetic hysteresis curve recorded at 300 k for Co_3O_4–Fe_3O_4 hybrid nanoparticle (CoFNP) with Fe_3O_4 nanoparticles (FeONP)

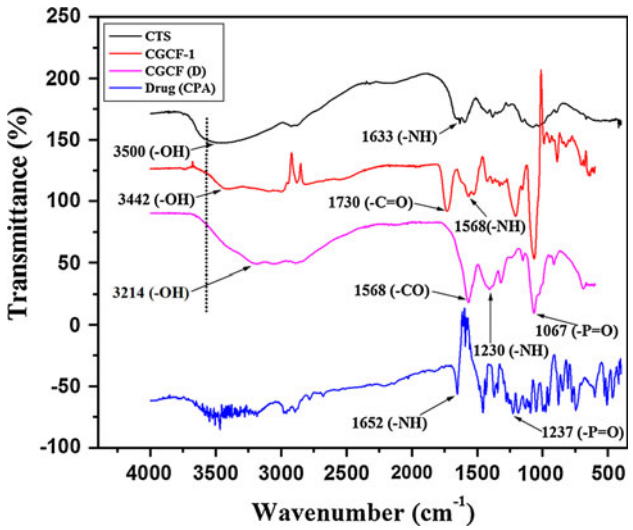

Fig. 3 FTIR spectra of neat chitosan (CTS), grafted chitosan (CGCF-1), grafted chitosan, and Co_3O_4–Fe_3O_4 hybrid nanoparticle-based nanohybrid scaffold (CGCF-(D)) and drug cyclophosphamide (CPA)

Physical property measurement system (PPMS) analysis

The magnetic properties of the hybrid nanoparticle were investigated to evaluate the influence of the diamagnetic Co_3O_4 on the Fe_3O_4 domains. Figure 2 shows the magnetic hysteresis loops recorded at 300 k of Co_3O_4–Fe_3O_4 hybrid nanoparticle with Fe_3O_4 nanoparticle of size 5–10 nm. Hybrid nanoparticles are super paramagnetic; however, the saturation magnetization increases with Co_3O_4 particles [29]. The decrease in the magnetization of Co_3O_4–Fe_3O_4 hybrid nanoparticle confirms the formation of Co_3O_4–Fe_3O_4 hybrid nanoparticles.

FTIR analysis

Fourier transform infrared (FT-IR) spectra reveals information about the structure of neat chitosan (CTS), chitosan grafted glycolic acid (CGCF-1), nanohybrid scaffold (CGCF-(D)), and drug (CPA) (Fig. 3). The characteristic peaks in the FTIR spectrum of CTS include 1633 cm^{-1} (–NH stretching) and 3500 cm^{-1} (–OH stretching). The presence of extra peak in CGPF-1at 1730 cm^{-1} corresponds to –C=O stretching of anhydride bond which is formed due to the polycondensation between the glycolic acid molecules during grafting process. Shifting of peak (–NH stretching) toward the lower frequency region (1568 cm^{-1}) confirms the interaction of glycolic acid with NH_2 group of chitosan. The grafting of glycolic acid on chitosan was confirmed by the formation of amide (–NH–C=O) linkage between amine (–NH_2) group of chitosan and –C=O group of glycolic acid. The FTIR spectra of CPA include peaks at 1237 cm^{-1} (–P=O stretching) and 1652 cm^{-1} (–NH stretching). The FTIR spectra of CGCF-(D) include shift in peaks 1067 cm^{-1} (–P=O stretching) and 3214 cm^{-1} (–OH stretching), which may be due to the interaction of Co_3O_4–Fe_3O_4 hybrid nanoparticles with –P=O group of drug molecule and –OH group of chitosan via metallic bond. The peak at 1568 cm^{-1} in CGCF-(D) is attributed to the shift in –C=O stretching toward lower frequency region, which may be due to the interaction of

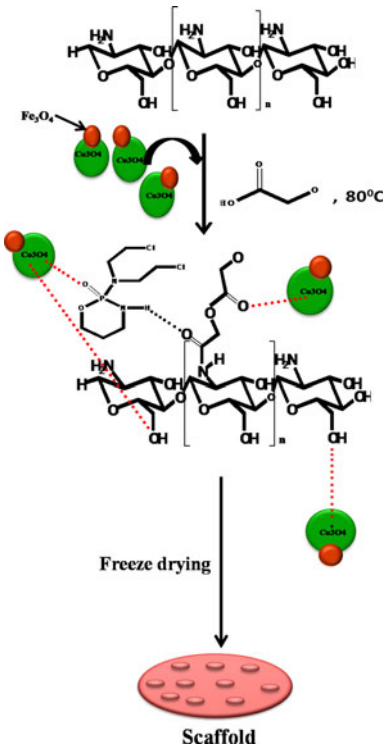

Scheme 1 Grafting of glycolic acid on chitosan, formation of CS-g-glycolic acid and Co_3O_4–Fe_3O_4 hybrid nanoparticle-based nanohybrid scaffold, and the interaction between chitosan-g-glycolic acid, drug, and Co_3O_4–Fe_3O_4 hybrid nanoparticles

CPA with –C=O group of grafted glycolic acid via H- bonding (Scheme 1).

XRD analysis

Figure 4a illustrates the X- ray diffraction pattern of neat chitosan (CTS) and glycolic acid-grafted chitosan (CGCF-1). It was observed that neat chitosan (CTS) shows the characteristic peaks at 10.9° and 19.8°, which correspond to a hydrated crystalline structure and an amorphous structure of chitosan, respectively [31–33]. Grafting of chitosan with glycolic acid (CGCF-1) resulted in a shift of peak from 10.9° to 10.1° and from 19.8° to 20.6°, confirming the interaction of chitosan with glycolic acid. These peaks were shifted from 10.1° to 8.1° and from 20.6° to 22.5°, showing the interaction of Co_3O_4–Fe_3O_4 hybrid nanoparticles with the grafted chitosan (CGCF-2) as shown in Fig. 4b.

SEM observation of scaffolds

The SEM image (Fig. 5a, b) reveals the morphology of nanohybrid scaffold before drug loading and after drug addition (Fig. 5c, d). It is observed that the pore size of scaffold before drug addition was ranging from 30.10 to

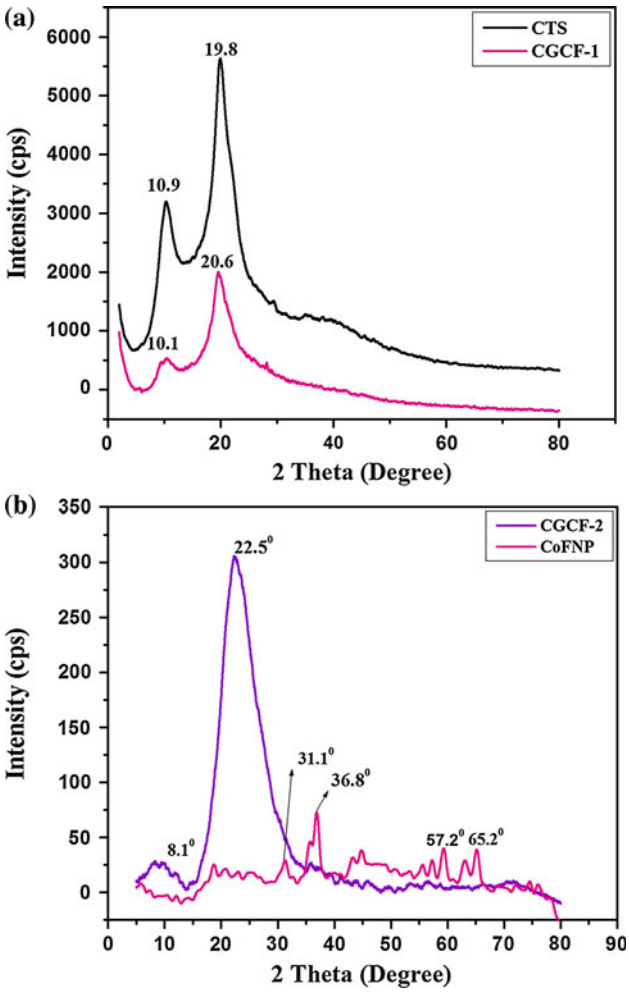

Fig. 4 **a** X-ray diffraction spectra of neat chitosan and grafted chitosan. **b** X-ray diffraction spectra of CS-g-glycolic acid and Co_3O_4–Fe_3O_4 hybrid nanoparticle-based nanohybrid scaffold

40.10 μm; however, upon the addition of drug, pore size decreases and lies in the range of 12.87–11.07 μm. The decrease in the pore size may be due to the incorporation of drug molecule in the pores of scaffold. The peaks of cobalt (Co), iron (Fe), and oxygen (O) in SEM-EDAX of scaffold (CGCF-(D)) were observed, which confirms the incorporation of Co_3O_4–Fe_3O_4 hybrid nanoparticles in nanohybrid (Fig. 5e).

Drug delivery study

Figure 6 shows the cumulative drug release versus immersion time of drug-loaded scaffold (CGCF-(D)). In vitro drug release shows the burst effect [34] which was examined with SBF (pH 7.4) at temperature 37 °C. The release media was quantified by UV–visible spectral absorbance values. From the figure, it was observed that the drug release follows the first order release kinetics which states that the drug release rate depends on its

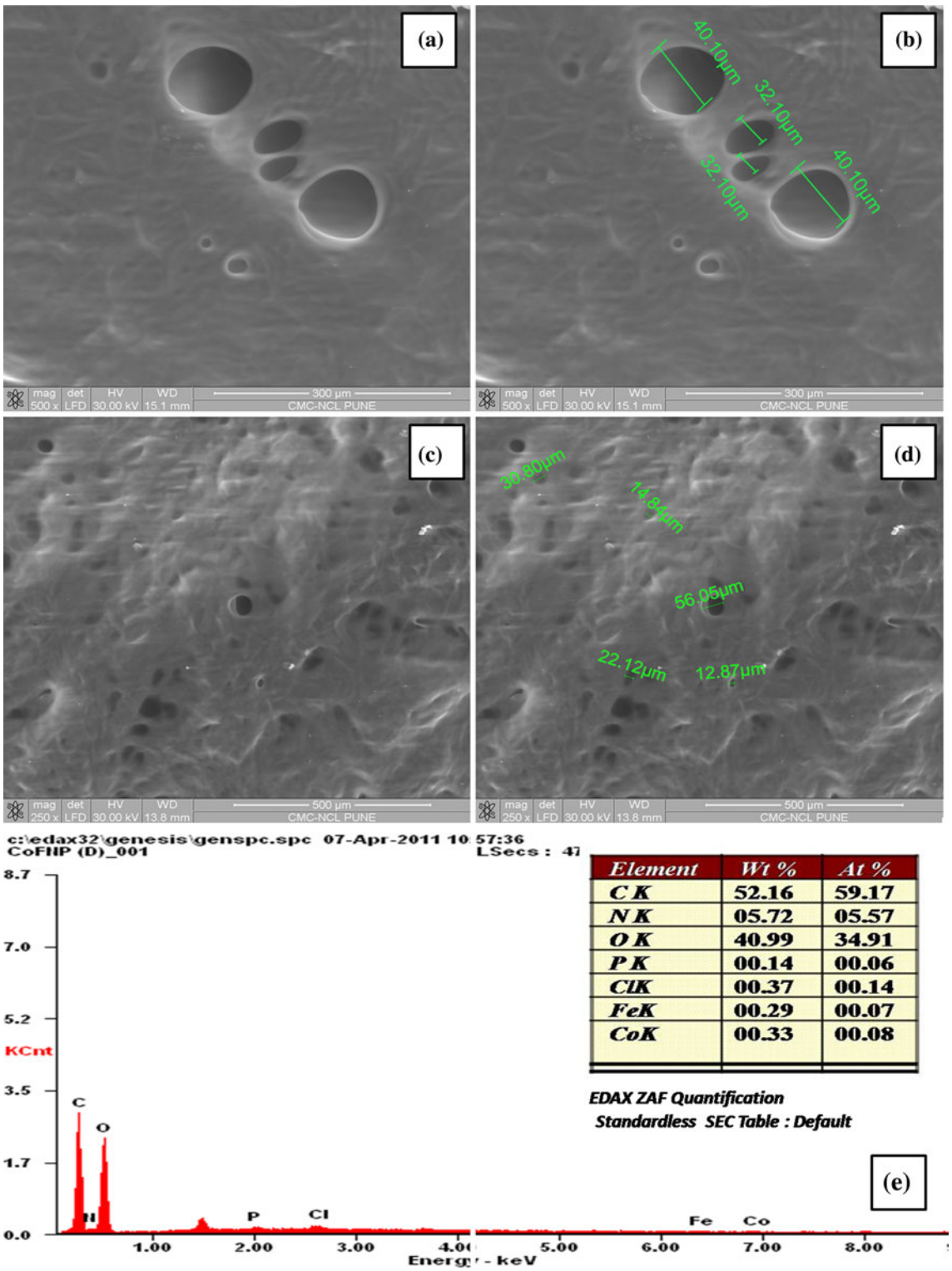

Fig. 5 **a**, **b** SEM image of grafted chitosan and Co_3O_4–Fe_3O_4 nanohybrid scaffold without drug; **c**, **d** SEM image of grafted chitosan and Co_3O_4–Fe_3O_4 nanohybrid scaffold with drug; **e** EDAX of nanohybrid scaffold (CGCF-(D))

concentration. Initially, the rate of the release of drug was high and it decreases with time because the drug which is at the surface of scaffold is released much faster than the drug incorporated deeply into the pores of the scaffold. The effect of incorporation of Co_3O_4–Fe_3O_4 hybrid nanoparticles can be significantly observed as reduced rate of release

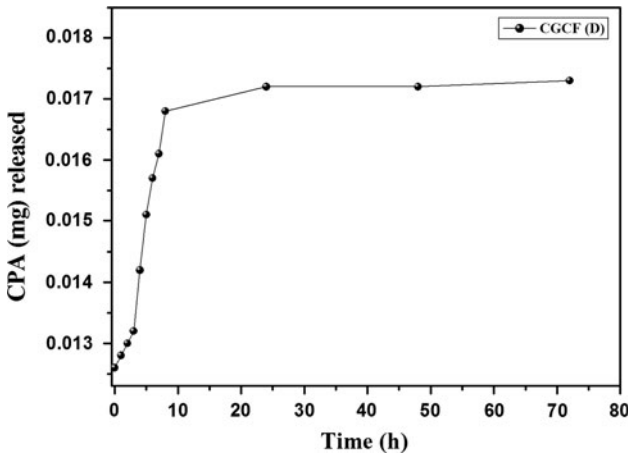

Fig. 6 Cumulative drug release profile from the prepared nanohybrid scaffold (CGCF-(D)) at pH = 7.4 and at temperature $T = 37$ °C

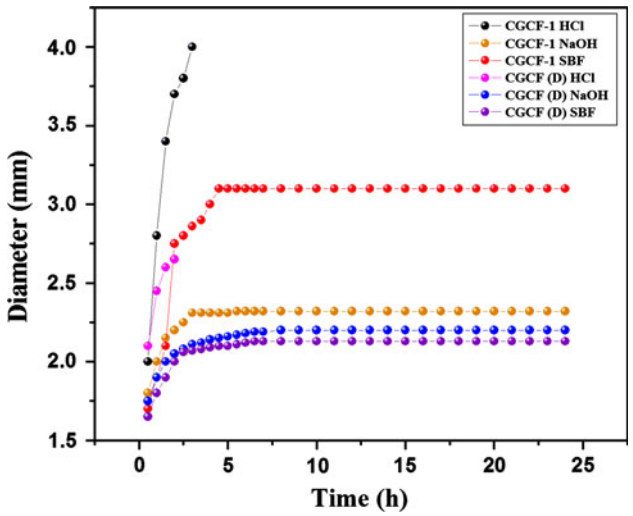

Fig. 7 Shape retention of scaffolds prepared from grafted chitosan and Co_3O_4–Fe_3O_4 nanohybrid

at initial stage of immersion (up to 200 min). Initially, the specimen is solvated, which facilitates the lateral diffusion of drug after 250 min [35]. The rate of release of drug decrease over the time, which may be due to the interaction of Co_3O_4–Fe_3O_4 composite nanoparticles and grafted glycolic acid chains with the loaded drug [31]. The release of drug at different temperature and pH is shown and discussed in Supplementary material (Fig. S1a, b, c, d, e, f).

Swelling behavior

In general, the swelling of chitosan involves the protonation of amino/imine groups and the mechanical relaxation of coiled chitosan chain [33, 36]. Shape retention was studied by measuring the change in the diameter as a function of immersion time in the media [37]. Swelling behavior of scaffold strongly depends upon the pH of the implantation site for their practical use in tissue engineering. It was investigated by exposing it to the media at different pH—1 N HCl (pH 1.2), 1 N NaOH (pH 14), and simulated body fluid (SBF) (pH 7.4) solutions for 24 h. The in vitro cell culture studies indicate that initial swelling is desirable [38, 39], but continuous swelling reduces the mechanical integrity and leads to the generation of compressive stress to the surrounding tissue. It is observed that scaffold CGCF (S) dissolve completely in the HCl solution within 2.5 h of immersion, whereas the rate of swelling is very low in NaOH and reached the plateau level around 3 h of immersion; however, the increase in size of scaffold is observed within 6 h in SBF solution. In the case of scaffold CGCF-(D), its complete dissolution was observed in HCl solution within 2.5 h of immersion, whereas slight swelling was observed in SBF within 3.5 h. These results showed that nanohybrid scaffold is stable toward the SBF and higher pH solution (Fig. 7).

Cell viability study

MTT assay was carried out to evaluate the proliferation of L929 on (CGCF-(D)). It is observed that cell viability on scaffold is decreased during first the 2 h. It may be because during proliferation cells have occupied all the available spaces on the scaffold [40]. Present study implies that the cell proliferation is not affected by the incorporation of Co_3O_4–Fe_3O_4 composite nanoparticles into glycolic acid-grafted chitosan [36]. This may be due to the enhanced interaction between Co_3O_4–Fe_3O_4 composite nanoparticles and growing cells on the biopolymer matrix (Fig. 8a). These results of improved cell proliferation and cell adherence on scaffold was mainly due to the presence of reactive groups on the polymer surface and improved hydrophilicity after hydrolysis, similar to those reported by other researchers [41]. It is observed that during the cell viability study, the morphologies of the cells are not changed much (Fig. 8b). The Co_3O_4–Fe_3O_4 composite nanoparticles may develop London–van der Waals forces with cells. These Co_3O_4–Fe_3O_4 composite magnetic nanoparticles can act as adhesives between biopolymer and cells through hydrogen bonding between the hydroxyl groups of chitosan and slight hydrophilic behavior of Co_3O_4–Fe_3O_4 composite magnetic nanoparticles .

Conclusion

The present study examined the potential use of hybrids of chitosan-g-glycolic acid and Co_3O_4–Fe_3O_4 composite magnetic nanoparticles as biomaterial. The FTIR confirmed the interaction of cationic chitosan with

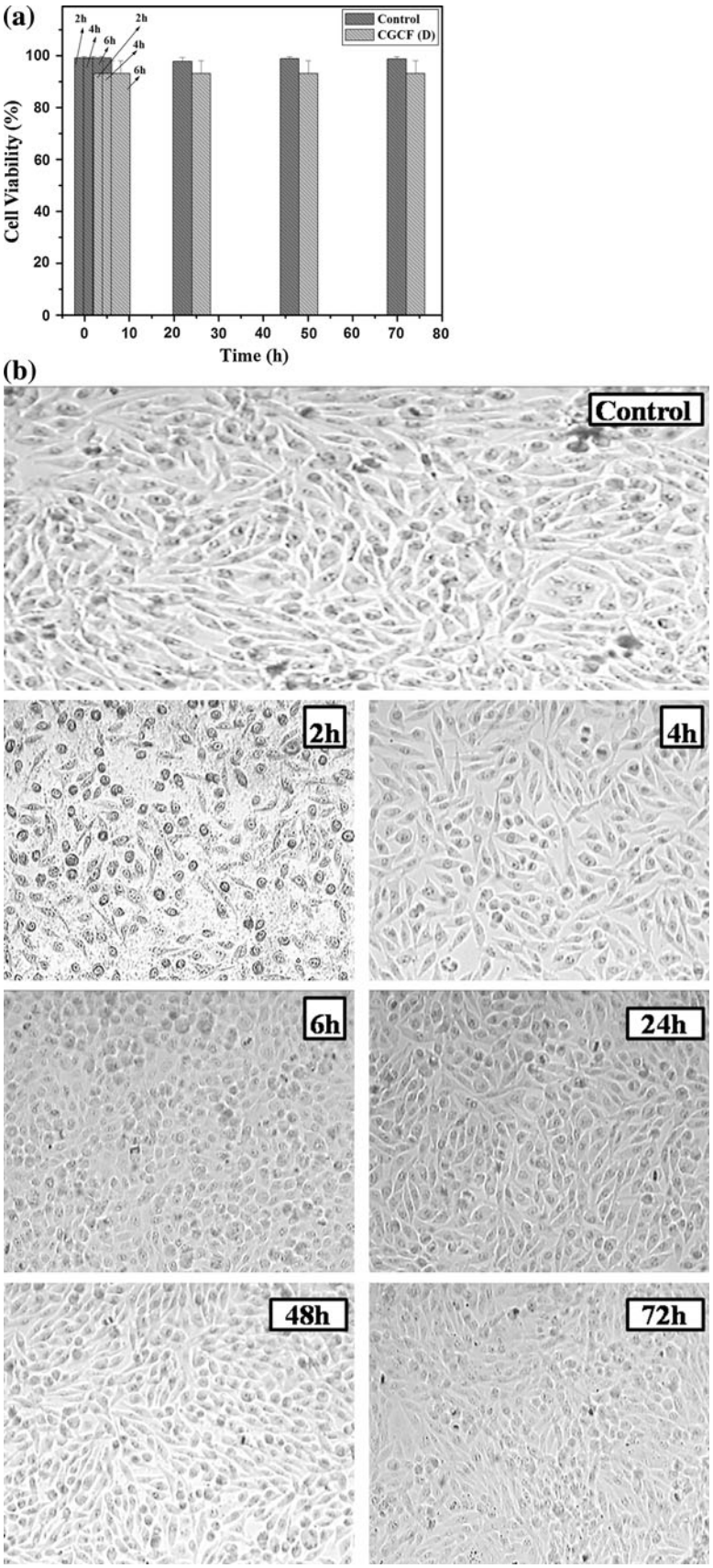

Fig. 8 **a** Cell viability study done by MTT assay of cultured cells. **b** Cell morphology at different time interval

Co_3O_4–Fe_3O_4 composite nanoparticles via metallic bond and linkage of drug with the polymer matrix via H-bond. The nanohybrid scaffolds are stable regardless of the pH of the medium. The nanohybrid scaffold possess porous morphology. The porous nanohybrid scaffolds have shown faster and higher drug release. The incorporation of Co_3O_4–Fe_3O_4 composite nanoparticles was observed to control the initial release of drug. From the results, we conclude that the prepared nanohybrid scaffold is biocompatible and also Co_3O_4–Fe_3O_4 composite magnetic nanoparticles are viable additives for formulating sustained drug delivery systems and could be applied in the field of biomaterials.

Acknowledgements We are grateful to Dr. Saurav Pal, Director, National Chemical Laboratory, Pune, India, for his fruitful discussions and suggestions. S.K is thankful to the Council of Scientific and Industrial Research (CSIR), New Delhi, India, for granting junior research fellowship.

References

1. Chapman R, Mulvaney P (2001) Chem Phys Lett 349:358
2. Krishnamoorti R, Vaia RA (2002) Polymer nanocomposites. ACS, Washington, DC, p 159
3. Lagaly G (1999) Appl Clay Sci 15:1
4. Luckham PF, Rossi S (1999) Adv Colloid Interface Sci 82:43
5. Jin R (2010) Nanoscale 2:343
6. Alvarez MM, Khoury JT, Schaaff TG, Vezmar I, gullin MNS, Whitten RL (1997) J Phys Chem B 101:3706
7. Zhu M, Aikens CM, Hollander FJ, Schatz GC, Jin R (2008) J Am Chem Soc 130:5883
8. Teranishi T (2003) Comptes Rendus Chimie 6:979
9. Pastoriza-Santos I, Gomez D, Pérez-Juste J, Luis M, Liz-Marzán LM, Mulvaney P (2004) Phys Chem Chem Phys 6:5056
10. Yamamoto Y, Miura T, Nakae Y, Teranishi T, Miyake M, Hori H (2003) Phys B 329:1183
11. Aiken JD III, Finke RG (1999) J Mol Catal A 145:1
12. Roucoux A, Schulz J, Patin H (2002) Chem Rev 102:3757
13. Bradley JS, Schmid G (2004) Nanoparticles. Wiley-VCH, Weinheim, p 186p
14. Akiyama S, Yoshimura T, Esum K (2005) J Jpn Soc Colour Mater 78:112
15. Jiang Y, Zhang L, Yang D, Li L, Zhang Y, Li J, Jiang Z (2008) Ind Eng Chem Res 47:2495
16. Jiang Y, Yang D, Zhang L, Sun Q, Sun X, Li J, Jiang Z (2009) Adv Funct Mater 19:150
17. Liu X, Qiu G, Li X (2005) Nanotechnology 16:3035
18. Souza KC, Ardisson ÆJD (2009) J Mater Sci 20:507. doi: 10.1007/s10856-008-3592-1
19. Duncan R (2003) Nat Rev Drug Discov 2:347
20. Duncan R (2006) J Drug Target 14:333
21. Torchilin V (2008) Drug Deliv 5:1003
22. Sampathkumar SG, Yarema K (2005) J Chem Biol 12:5
23. Van TN, Ng CH, Aye KN, Trang TS, Stevens WF (2006) Chem Technol Biotechnol 81:1113
24. Xie M, Liu HH, Chen P, Zhang ZL, Wang XH, Xie ZX, Du YM, Pand BQ, Pang DW (2005) Chem Commun 44:5518
25. Xie J, Zhang Q, Lee JY, Wang DIC (2008) ACS Nano 2:2473
26. Dos Santos JDS, Goulet PJG, Pieczonka NPW, Oliveira ON, Aroca RF (2004) Langmuir 20:1027
27. Kurita K (2001) Prog Polym Sci 26:1921
28. Hong RL, Yu JY (2004) J Biomed Mater 71B:52
29. Schladt TD, Shukoor MI, Schneider K, Tahir MN, Natalio F, Ament I, Becker J, Jochum FD, Weber S, Köhler O, Theato P, Schreiber LM, Sönnichsen C, Schröder C, Müller WEG, Tremel W (2010) Angew Chem 49:3976
30. Takahashi T, Yamaguchi M (1991) J Colloid Interface Sci 146:556
31. Rhim JW, Seok INH, Park HM, Perry KWNG (2006) J Agric Food Chem 54:5814
32. Mei Y, Zhao Y (2003) J Agric Food Chem 51:1914
33. Park SI, Zhao Y (2004) J Agric Food Chem 52:1933
34. Xiao H, Christopher SB (2001) J Control Release 73:121
35. Shilin L, Haoze H, Jinping Z, Lina Z (2011) Cellulose 18:1273
36. Vachoud L, Zydowicz N, Domard A (2000) Carbohyd Res 326:295
37. Aiba S (1991) Int J Biol Macromol 13:40
38. Kumari S, Singh RP (2012) Int J Biol Macromol 50:878
39. Liz-Marzan LM (2004) Mater Today 7:26
40. Shanmugasundram N, Ravichandaran P, Reddy PN, Ramamurth N, Pal S, Rao KP (2001) Biomaterials 22:1943
41. Chen F, Lee CN, Teoh SH (2007) Mater Sci Eng C 27:325